CFD-Dose Comprehensive Mentorship

# Applied Project: Particle Deposition Prediction in a 90-Degree Bend

## Simulated Using T-Flows CFD Software

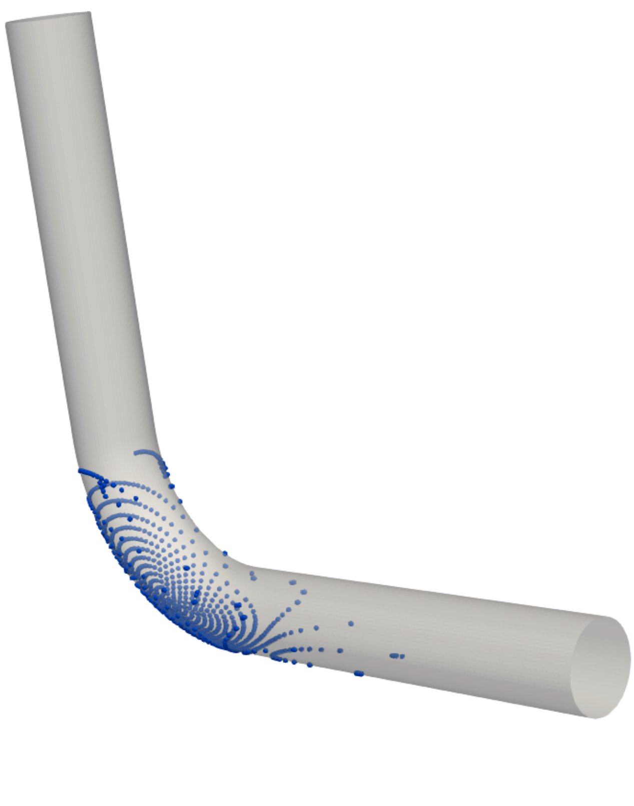


Author: Selim SHERIF


January 29, 2025

# Contents

# 1 Overview

Curved geometries, such as those found in pneumatic transport systems, ventilation ducts, and exhaust lines, are integral to many industrial applications. These configurations often introduce complex secondary flows, accompanied by swirling structures, which significantly influence particle motion. Understanding and predicting these behaviors is essential for optimizing system design, enhancing efficiency, and minimizing maintenance requirements.

This study leverages the academic `T-Flows` CFD software to simulate particle-laden flow through a 90° pipe bend, focusing on accurately capturing particle deposition patterns. By establishing a robust workflow, the project aims to:

- Model fluid flow and turbulence in the pipe-bend geometry.
- Inject inert particles of varying sizes into the flow.
- Analyze how particle trajectories and deposition vary with particle diameter.

The ultimate objective is to generate a size-deposition curve and validate the simulation results against experimental and numerical benchmarks. This approach not only tests the capabilities of `T-Flows` but also provides deeper insights into particle transport phenomena, contributing to the broader understanding of such systems in industrial contexts.

# 2 Governing Equations and Assumptions

`T-Flows` solves the incompressible, unsteady Navier-Stokes equations for the continuous (fluid) phase under Reynolds-Averaged Navier-Stokes (RANS) or Large-Eddy Simulation (LES) modeling:

- **Continuity:**
$$\nabla \cdot \mathbf{u} = 0,$$
- **Momentum:**
$$\frac{\partial \mathbf{u}}{\partial t} + \nabla \cdot \big(\mathbf{u} \otimes \mathbf{u}\big) = -\frac{1}{\rho}\nabla p + \nu \nabla^2 \mathbf{u} + \mathbf{f}_{\mathrm{turb}},$$

where $\mathbf{u}$ is velocity, $\rho$ is density, $p$ is pressure, and $\nu$ is kinematic viscosity. Turbulence effects are incorporated through $\mathbf{f}_{\mathrm{turb}}$, depending on the chosen RANS or LES closure.

For the dispersed (particle) phase, `T-Flows` adopts a Lagrangian tracking method with the following assumptions:

- Incompressible, Newtonian fluid with constant density and viscosity.
- Spherical particles of fixed diameter (per run), with a density significantly higher than the fluid.
- One-way coupling only: Particle loading does not alter the fluid flow field.

# 3 Geometry and Domain Setup

## 3.1 Overarching Setup

The computational setup consists of two connected domains to ensure a fully developed flow enters the bend:

1. **Straight Pipe (Development Region):** A cylindrical inlet domain aligned with the $y$-axis, where mass-flow or pressure-drop conditions drive the flow. Specifically:

```
PRESSURE_DROPS       0.0  -9.0    0.0
MASS_FLOW_RATES      0.0  -9.42e-4  0.0
```

2. **Bend Region:** A 90° curved pipe connected to the straight pipe. Particles primarily deposit here due to curvature-induced secondary flows.

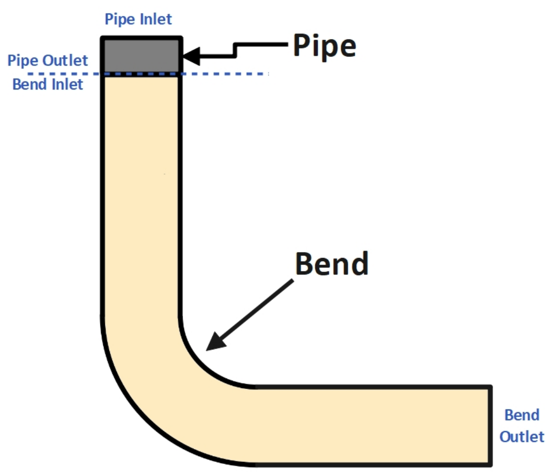


Figure 1: Schematic of the computational domains: (1) Straight Pipe (Development Region) and (2) 90° Bend Region.

An **Interface Condition** enforces a seamless connection, mapping the pipe outlet to the bend inlet:

```
INTERFACE_CONDITION       pipe         bend
    BOUNDARY_CONDITIONS     periodic_y    bend_inlet
```

## 3.2 Mesh

The mesh used in this simulation is identical to the one utilized in [1]. It features a structured hexahedral configuration with refinement in critical regions, particularly near the pipe walls and the bend area, to accurately capture boundary layer effects and secondary flow structures. The following image illustrates the cross-sectional view of the mesh at the pipe inlet, highlighting the structured and uniform grid distribution:

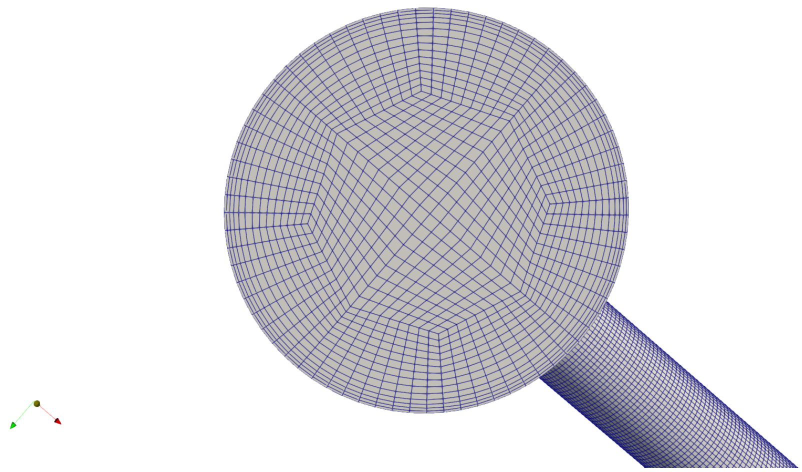

Figure 2: Cross-sectional view of the structured mesh used in the simulation.

# 4 Case Parameters and Settings

## 4.1 Physical Modeling Properties

The fluid properties for the carrier phase are essential for accurate simulation results. Table 1 lists the key parameters used in this study:

Table 1: Fluid properties for the carrier phase.

| **Property** | **Value** |
|---|---|
| Density, $\rho$ | $1.2\,\mathrm{kg\,m^{-3}}$ |
| Dynamic Viscosity, $\mu$ | $1.8 \times 10^{-5}\,\mathrm{Pa\,s}$ |
| Turbulence Parameter, $k_\epsilon$ | *Value not specified* |

These fluid properties are used throughout the simulations to calculate flow dynamics, turbulence characteristics, and energy dissipation rates.

## 4.2 Boundary Conditions and Initial Conditions

### Boundary Conditions

The boundary conditions used for both the pipe and the bend are specified below, noting again the periodic interface from the pipe outlet to the bend inlet:

Listing 1: Boundary conditions for the simulation domains.

```
BOUNDARY_CONDITION    pipe_walls
    TYPE                wall
    VARIABLES           u     v     w
    VALUES              0.0   0.0   0.0

BOUNDARY_CONDITION    bend_walls
    TYPE                wall
    VARIABLES           u     v     w
    VALUES              0.0   0.0   0.0

BOUNDARY_CONDITION    bend_inlet
    TYPE                inflow
    VARIABLES           u     v     w
    VALUES              0.0   -3.0  0.0

BOUNDARY_CONDITION    bend_outlet
    TYPE                outflow
    VARIABLES           u     v     w
    VALUES              0.0   0.0   0.0

INTERFACE_CONDITION      pipe          bend
    BOUNDARY_CONDITIONS    periodic_y    bend_inlet
```

### Initial Conditions

The initial conditions are the same throughout both domains and are specified below:

Listing 2: Initial conditions for both domains.

```
INITIAL_CONDITION
    VARIABLES           u     v     w     kin    eps    zeta   f22
    VALUES              0.0   0.0   0.0   0.01   0.001  0.1    0.1
```

### 4.3 Workflow of Simulation

The simulation workflow consists of two primary stages:

**Flow Development $\longrightarrow$ Particle Tracking and Lagrangian Simulation**

#### 4.3.1 Flow Development

To establish a stable velocity field, the flow is first developed **without particle tracking**. The simulation is integrated for five seconds using a time step of 0.005 s, resulting in 1000 total time steps:

```
TIME_STEP            0.005
NUMBER_OF_TIME_STEPS  1000
```

The solver employs a standard SIMPLE algorithm with the `minmod` momentum advection scheme. Detailed numerical parameters (including under-relaxation factors and solver tolerances) can be found in **Appendix A.1**. These settings are also used throughout all simulations.

#### 4.3.2 Particle Tracking

Once the flow is developed, particles are introduced via the `T-Flows` swarm feature. The simulation proceeds for an additional two seconds with:

```
TIME_STEP            0.0001
NUMBER_OF_TIME_STEPS  20000
```

A range of particle diameters is tested to assess deposition behavior. The tested swarm diameters are presented in Table 2.

Table 2: Tested Swarm Particle Diameters

| **Diameter ($\mu$m)** | 3 | 5 | 10 | 15 | 20 | 25 | 30 | 40 | 50 |
|---|---|---|---|---|---|---|---|---|---|

These particle sizes were selected to evaluate the influence of diameter on deposition patterns within the bend region and represent critical ranges that exhibit significant variability.

For more information about swarm parameters used, please refer to **Appendix A.2**.

## 5 Simulation Results

Figure 3 presents the outcomes of the simulation using different approaches compared against experimental data, which serves as the benchmark. The reference data for Fluent, T-Flows, and experimental benchmarks is sourced from the paper: *On the Capability of Wall-Modeled Large Eddy Simulations to Predict Particle Dispersion in Complex Turbulent Flows* [1].

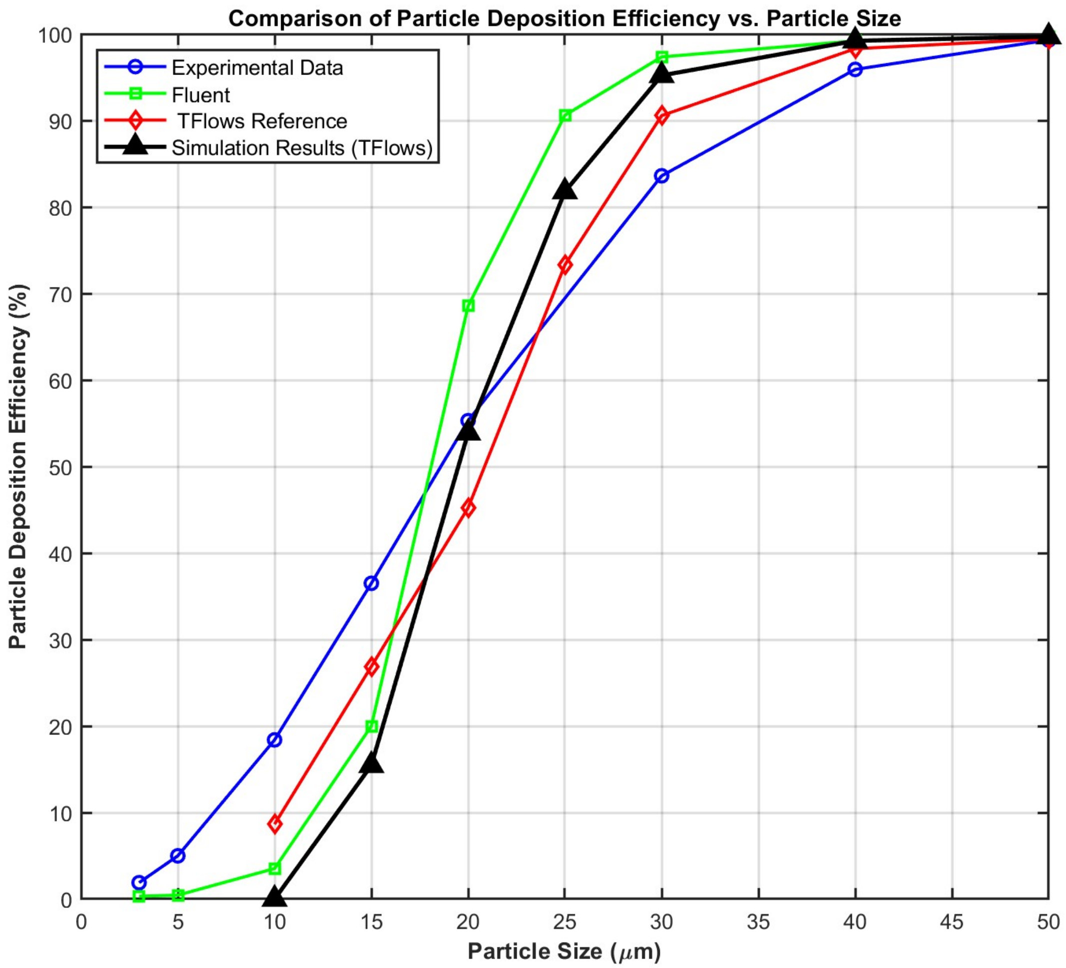


Figure 3: Comparison of simulation results with reference data from Fluent, T-Flows, and experimental benchmarks.

The numerical results are detailed in the annex for further reference B

## 5.1 Observations

- **T-Flows Reference Data:** The T-Flows reference data does not overlap with our simulation results. This is expected as the turbulence model used in our simulations is less sophisticated. The reference employs a hybrid RANS/LES model, while our simulation uses a standard $k$-$\varepsilon$ model.
- **Fluent Data:** The simulation data closely aligns with the Fluent reference data, which also employs a $k$-$\varepsilon$ model. Notably, our simulation data appears slightly shifted relative to the T-Flows reference data, with our model being more precise for larger particle sizes, while Fluent shows better agreement for smaller sizes.
- **Experimental Data:** The hybrid RANS/LES model shows the closest agreement with the experimental data, as expected due to its higher fidelity in capturing complex turbulence

phenomena.

### 5.2 Particle Size Visual Analysis

To gain a more intuitive feel for the behavior of different particle sizes, simulations were post-processed and visualized for $3\,\mu$m, $25\,\mu$m, and $50\,\mu$m. The sticking behavior and distribution of particles within the pipe are visualized in Figure 4, emphasizing the accumulation patterns, particularly at the neck of the pipe.

(a) **3 $\mu$m Particles:** No sticking. Small particles follow fluid streamlines, resulting in negligible wall interaction.

(b) **25 $\mu$m Particles:** Moderate sticking. Particles begin to accumulate, influenced by inertia, with noticeable adhesion along the neck and bend.

(c) **50 $\mu$m Particles:** Full accumulation. Larger particles experience strong inertial effects, leading to pronounced sticking at the neck of the pipe.

Figure 4: Particle distribution for different sizes inside the pipe. The neck of the pipe is the primary sticking region, with accumulation increasing as particle size grows.

## 6 Conclusion

This study utilized `T-Flows` CFD software to simulate particle deposition in a 90° pipe bend, revealing that larger particles exhibit increased deposition due to stronger inertial effects and curvature-induced secondary flows. The simulation results aligned closely with Fluent's $k$-$\varepsilon$ model for larger particle sizes, while discrepancies with T-Flows' hybrid RANS/LES data highlighted the impact of turbulence modeling choices.

## References

[1] Mohamed Aly Hashem Mohamed Sayed. "On the Capability of Wall-Modeled Large Eddy Simulations to Predict Particle Dispersion in Complex Turbulent Flows". EPFL Thesis No. 10054. PhD thesis. École Polytechnique Fédérale de Lausanne, 2022. URL: `https://infoscience.epfl.ch/record/298741`.

# A Simulation Control Parameters

## A.1 Flow-Related Parameters

```
PRESSURE_MOMENTUM_COUPLING    simple
SIMPLE_UNDERRELAXATION_FOR_MOMENTUM    0.6
SIMPLE_UNDERRELAXATION_FOR_PRESSURE    0.3
SIMPLE_UNDERRELAXATION_FOR_TURBULENCE  0.3
TIME_INTEGRATION_SCHEME  linear
ADVECTION_SCHEME_FOR_MOMENTUM     minmod
PRECONDITIONER_FOR_SYSTEM_MATRIX   incomplete_cholesky
TOLERANCE_FOR_MOMENTUM_SOLVER      1.e-3
TOLERANCE_FOR_PRESSURE_SOLVER      1.e-5
TOLERANCE_FOR_SIMPLE_ALGORITHM     1.e-3
MIN_SIMPLE_ITERATIONS              3
MAX_ITERATIONS_FOR_PRESSURE_SOLVER 480
GRADIENT_METHOD_FOR_PRESSURE       gauss_theorem
```

## A.2 Swarm-Related Parameters

```
PARTICLE_TRACKING                  yes
SWARM_DENSITY                      1000.0
NUMBER_OF_SWARM_SUB_STEPS          8
MAX_PARTICLES                      10000
SWARM_COEFFICIENT_OF_RESTITUTION   1.0
```

# B Numerical Results and Data

Table 3: Combined data from simulations and reference datasets for deposition size.

| Deposition Size | Experimental Data | Fluent Data | T-Flows Reference | Simulation Results |
|---|---|---|---|---|
| 3 | 1.9 | 0.3290 | 3.589 | 0.000 |
| 5 | 5.0 | 0.4525 | 3.717 | 0.000 |
| 10 | 18.4 | 3.5300 | 8.652 | 0.000 |
| 15 | 36.5 | 20.0000 | 26.896 | 15.452 |
| 20 | 55.3 | 68.5520 | 45.225 | 53.883 |
| 25 | NaN | 90.5980 | 73.296 | 81.775 |
| 30 | 83.6 | 97.3441 | 90.558 | 95.206 |
| 40 | 95.9 | 99.1955 | 98.291 | 99.208 |
| 50 | 99.3 | 99.6780 | 99.423 | 99.683 |